Development of a Large Field-of-View PIV System for Rotorcraft Testing in the 14- x 22-Foot Subsonic Tunnel

Luther N. Jenkins, Chung-Sheng Yao, Scott M. Bartram, Jerome Harris, and Brian Allan
NASA Langley Research Center, Hampton, Virginia

Oliver Wong
U.S. Army Joint Research Program Office, Aeroflightdynamics Directorate
NASA Langley Research Center, Hampton, Virginia

W. Derry Mace
Sierra-Lobo, Hampton, Virginia

Abstract

A Large Field-of-View Particle Image Velocimetry (LFPIV) system has been developed for rotor wake diagnostics in the 14-by 22-Foot Subsonic Tunnel. The system has been used to measure three components of velocity in a plane as large as 1.524 meters by 0.914 meters in both forward flight and hover tests. Overall, the system performance has exceeded design expectations in terms of accuracy and efficiency. Measurements synchronized with the rotor position during forward flight and hover tests have shown that the system is able to capture the complex interaction of the body and rotor wakes as well as basic details of the blade tip vortex at several wake ages. Measurements obtained with traditional techniques such as multi-hole pressure probes, Laser Doppler Velocimetry (LDV), and 2D Particle Image Velocimetry (PIV) show good agreement with LFPIV measurements.

Notation

b	wing half-span, 0.914 meter
C_T	rotor thrust coefficient
L	length of body, 1.757 meters
M_{tip}	tip Mach number
R	blade radius, meters
X,Y,Z	streamwise, spanwise, and vertical coordinate, meters
U,V,W	streamwise, spanwise, and vertical components of velocity, m/s
U_∞	freestream velocity, m/s
α	angle of attack, degrees
β	sideslip angle, degrees
Ω	angular velocity of rotor blade, (radians/s)
Ψ	blade azimuth, degrees
ω_X	streamwise vorticity, s^{-1}

Presented at the American Helicopter Society 65th Annual Forum, Grapevine, Texas, May 27-29, 2009.

Introduction

The development of new experimental techniques and capabilities is an integral component of rotorcraft research at NASA. Advances in measurement science and methods are used to increase understanding and insight, conduct performance assessments, validate predictive design tools, characterize new designs and concepts, and establish databases for developing design and analysis methods based on "first principles".

Many techniques being developed and used by NASA for rotorcraft research utilize laser, optical, and imaging techniques to measure flow properties non-intrusively, thereby avoiding potential collision hazards with the moving rotor and possible changes to the flow field due to the introduction of a physical probe. Although a considerable amount of the time is often required for setup, these optical techniques can be highly effective in providing both qualitative and quantitative information about the complex

flows produced by rotorcraft.

One area of flow which has considerable complexity is the rotor wake. This region is characterized by such features as blade tip vortices, vortex sheets, induced flow from the main and tail rotors, and significant interaction with the fuselage and tail section. Detailed quantitative information about these complex flow interactions is necessary to fully understand the rotor aerodynamics and the correlation of off-body flow with the overall performance characteristics of the vehicle. It is also essential for performing more stringent assessments of predictive tools and methods. To obtain and provide this type of information for the research community, NASA is developing Particle Image Velocimetry (PIV) systems for rotor wake diagnostics in the National Full-Scale Aerodynamics Complex (NFAC) at NASA Ames and the 14- by 22-Foot Subsonic Tunnel (14x22) at NASA Langley[1]. In the NFAC, the initial goal is to document an area 4.27 meters wide by 1.22 meters high with sufficient spatial resolution to define the structure of the trailed blade tip vortex. In the 14x22, the initial goal is to document an area 1.83 meters wide by 0.91 meter high to resolve the wake behind fuselage-rotor combinations. Measuring flow velocities with high accuracy over such large areas is an extreme challenge and requires the use of a relatively new measurement technique called *Large Field-of-View Particle Image Velocimetry (LFPIV)*.

This report describes the development and initial implementation of a stereoscopic (3D) LFPIV system for the 14x22. The system was applied in two rotorcraft tests, which provided a diverse set of test conditions for characterizing and evaluating system performance. Sample results from the two applications are presented along with recommendations for future development and enhancements.

Brief History of Large Field PIV Systems

For many years Laser Doppler Velocimetry (LDV) was the primary non-intrusive technique for rotor wake measurements. Although it proved to be quite useful as a diagnostic tool and provided quantitative information for developing rotor wake theories, its use in large wind tunnels and test facilities has not been widespread due to concerns regarding its efficiency. In most cases, the technique requires several minutes to acquire enough samples for statistical significance. Because this is done one point at a time, run times can be quite long. To improve efficiency while maintaining scope and accuracy, planar velocity measurement techniques such as PIV have been pursued.

PIV has been used extensively in a variety of fluid dynamics experiments and in numerous studies involving fixed wing vehicles; however, the use of PIV in rotorcraft research has been limited. This was due in large part to the size of digital camera sensors and resolution requirements of the technique which limited the size of the measurement area, also known as the field-of-view (FOV), to approximately 0.3 meter by 0.3 meter. This made it appropriate for measuring blade tip vortices on small, isolated rotors[2-4], but inefficient for capturing the evolution of the wake when rotor diameters exceed 1 meter. Applying PIV systems with a 0.3 meter by 0.3 meter FOV in these situations involves the costly and very time-consuming task of repositioning the cameras to cover the required measurement area. Increases in camera sensor size and a commensurate increase in the number of pixels have now made it possible to enlarge the FOV and capture a large portion of the rotor wake without sacrificing resolution. Known as Large Field-of-View PIV systems, these systems have been developed and implemented in a variety of test facilities. LFPIV has been used in both the Army Hover Chamber[5] and 7-ft x 10-Ft Wind Tunnel at NASA Ames Research Center where flow fields as large as 0.91 meter x 1.82 meters have been routinely measured[6-8]. In addition to these applications, an attempt was made in 2001 to apply the LFPIV technique in the NFAC 40-ft x 80-ft wind tunnel during testing of the Full-Span Tilt-Rotor Aeroacoustic Model (FS TRAM). Although the test ended prematurely due to model hardware issues, sufficient information was acquired to show the feasibility of using LFPIV in the NFAC despite the challenges of seeding the facility and the long distances over which the cameras and lasers were required to operate. European researchers have also used the technique to measure blade-tip vortices during the HART II Test in Germany's DNW Wind Tunnel[9]. Due to the success of these applications, LFPIV has emerged as a state-of-the-art technique for rotorcraft flow-field measurements. This has led to numerous research efforts, such as the current one, to improve its scope, efficiency, and accuracy.

System Development and Description

Design Criteria

Prior to developing the LFPIV system, the following criteria were established to guide the design and development process. Although LFPIV can be used for both fixed-wing and rotary-wing applications, many of these requirements are specific to rotorcraft testing and anticipated test conditions within the 14x22.

1. *The 14x22 test section will be configured with the tunnel walls up and ceiling down for optimal optical access.*
2. *The field of view or size of the measurement area should be at least 1.83 meters wide by 0.91 meter high.*
3. *Stereoscopic PIV will be used to measure three velocity components at working distances between 6.096 meters and 12.192 meters.*
4. *The initial development stage will focus on measuring the average rotor wake.*
5. *Measurement of the wake (velocities) must be synchronized with rotor position.*
6. *Accuracy of the prototype system should be comparable to existing single point measurement techniques.*

In addition to these requirements, an objective was established for the LFPIV system to achieve a level of performance comparable to laboratory-scale PIV systems (i.e. field-of-view < 0.5 *meters*) in terms of imaging the particles, seeding, calibration, and image processing. Laboratory scale PIV systems are routinely used to acquire critical data for CFD code development and validation so this was considered to be an appropriate benchmark. To meet this objective as well as the overall requirements of the system, significant technical challenges had to be considered.

System Components

The LFPIV system is an amalgamation of commercially available components from a variety of manufacturers. The system consists of a two Nd-Yag lasers, two 11 megapixel digital video cameras with external electromechanical shutters, framegrabber boards, large format lenses, and software for image acquisition and processing. With the exception of the large format cameras and lenses, these components are common to most PIV systems.

To maximize spatial resolution, two digital cameras featuring the KAI-110000CM interline transfer CCD sensor were selected. The camera provides a resolution of 4008 pixels by 2672 pixels and has a maximum frame rate of 4.63 frames per second. Each pixel measures 9.0 microns by 9.0 microns and has an output bit depth of 12-bits per pixel. Instead of a fan, the camera uses Peltier cooling to minimize dark noise and thermal drift. Camera control and data exchange with the data acquisition computer were accomplished using a framegrabber with a CameraLink interface. The framegrabber is capable of transferring data at rates up to 700 Megabytes per second which allows data to be acquired at the maximum frame rate of the camera. Electromechanical shutters were attached to each camera to permit image acquisition in ambient light conditions and prevent multiple laser pulses from appearing on the second image buffer which has a longer integration time. Each camera was attached to a lens board and mounted in a large format camera outfit. This arrangement is reminiscent of the early film-based PIV systems and offers numerous benefits such as precise positioning, easy focusing, Scheimflug adjustment, and the use of large format lenses. Large format lenses produce an image which is much larger than the sensor and enable different areas of interest to be imaged by repositioning the sensor in the image plane of the lens. This capability can be used to make small adjustments during setup in lieu of moving the entire camera stand or base.

A software package called PIVACQ[10] was used for camera control and acquisition. This software, developed at NASA Glenn Research Center, interfaces with the cameras, lasers, and shutters through a timing interface box. The box can accept an external trigger which is required to synchronize the system with a spinning rotor. Images acquired using PIVACQ were reduced and analyzed using two commercial software programs and an in-house code for assessing image quality.

Implementation and Evaluation

The LFPIV system was implemented in two rotorcraft tests to evaluate system performance and identify potential areas for further development. The first application was a forward-flight test involving a Slowed-Rotor Compound Helicopter. This provided the unique opportunity to test the system with and without a

spinning rotor. The second application was on a ROBIN configuration[11] in hover in the Rotor Test Cell at NASA Langley. Collectively, these tests provided a good representation of the diverse and challenging conditions in which the LFPIV system would be required to operate.

Facility Description

The 14x22 is one of three primary facilities used by NASA for rotorcraft testing. The facility is a closed-return, subsonic wind tunnel with a maximum speed of 103 m/s and maximum dynamic pressure of 6.503 kilopascals. These conditions correspond to a freestream Mach number of 0.3 and unit Reynolds number of 0.64 million per meter. As the name implies, the test section is 4.27 meters (14 feet) by 6.71 meters (22 feet) and can be configured in a variety of ways for testing vertical/short takeoff and landing (V/STOL) configurations. Additional details and information can be found in reference 12.

For rotorcraft testing, the test section can be configured in three ways: closed on one side only, closed on two sides, and fully closed. When the test section is closed on one side, the tunnel sidewalls and ceiling are raised but the floor remains in place. Flow collectors at the rear of the test section channel the flow into the diffuser. When the test section is closed on two sides, the floor is in place and the ceiling remains down to facilitate the use of the Isolated Rotor Test System (IRTS). With this arrangement, rotors can be tested in hover or forward flight with and without a fuselage present. Most tests in the facility are conducted with the test section fully closed.

Forward Flight Application: Slowed-Rotor Compound Helicopter Test

Background

The Slowed-Rotor Compound Helicopter Test was conducted jointly between NASA and the U.S. Army in 2007 on a notional, heavy-lift helicopter configuration in the 14x22. The objectives for the test were threefold: 1) to investigate the interactional aerodynamics of a large, slowed rotor on a compound configuration with a large wing mounted high on the fuselage, 2) to investigate effects of rotor/body separation distance on rotor wake geometry, and 3) to evaluate the LFPIV system.

The Slowed-Rotor Compound Helicopter model, shown in Figure 1, consisted of a body and rotor. The body measured 1.757 meters long and had a wing with a span measuring 1.828 meters. It was attached to an internal strain gauge balance mounted on a post that could be raised and lowered to change the height of the body. The four-bladed rotor had a radius of 0.897 meters with each blade having non-uniform twist, a tapered planform and a swept tapered tip. The root chord for each blade measured 0.057 meter and tip chord measured 0.035 meter. The rotor was attached to the IRTS which extends from the tunnel ceiling and contains the rotor balance. This arrangement permits the distance between the rotor and the body to be adjusted. The model was mounted in the center of the front test section which placed it 5.410 meters from the tunnel inlet. Since IRTS was being used, the tunnel floor and ceiling were in place but the sidewalls were raised which afforded unrestricted optical access from both sides of the tunnel.

Before the LFPIV system was installed in the tunnel, several activities were undertaken that significantly reduced installation time and proved crucial to the implementation. The first activity involved performing computations on the body alone using the flow solver code, OVERFLOW[13,14]. The results were used to identify major flow structures in the wake and to determine the optimum measurement locations to capture them. Once the measurement locations were determined, the second activity involved using the Virtual Diagnostics Interface (ViDI) tool[15] to examine the field-of-view obtained from various camera positions using lenses with different focal lengths. It is estimated that knowing the general camera positions and appropriate lenses a priori helped reduce the set up time by at least two days. The third activity involved making measurements in the wake behind the body alone at several flow conditions and angles of attack using the Boeing Quantitative Wake Survey System (QWSS)[16]. The system shown in Figure 2 consists of a multi-hole probe connected to a two-arm articulating support system that traverses the probe along an arc. Individual pressures are measured at each port using high-frequency pressure transducers and then combined using the calibration to compute total pressure, static pressure, three components of velocity, and flow angles. Although the primary purpose for using the QWSS was to provide redundant measurements for comparison with the LFPIV system, the results were also used to confirm the position of major flow structures and establish the datum for the calibration target. Comparisons

between QWSS and LFPIV measurements will be discussed using sample results from the body alone.

System Setup

The process of installing the hardware and preparing the system to acquire data involved setting up the cameras, producing the light sheet, calibrating the cameras, and verifying the performance of the seeding system. The camera heads, shutters, and lenses were installed in view camera mounts and mounted on heavy duty camera stands. The stands were positioned on the south side of the tunnel between the wall and the free shear layer formed at the tunnel inlet. Figure 3 shows the camera stands positioned upstream and downstream of the model. The figure also shows the LDV traverse and calibration target positioned behind the model at the location of the initial measurement plane.

The light sheet for this first application was generated using two 600 milliJoule Nd-Yag lasers. Each laser had a repetition rate of 10 Hz and beam diameter of 9 mm. The beams from each laser were combined and passed through a pair of cylindrical lenses to control the light sheet thickness. A third cylindrical lens was used to produce sufficient vertical spread to illuminate the measurement plane.

To calibrate the cameras, a calibration target was assembled using a 6.35 mm thick perforated sheet measuring 1.22 meters high by 2.44 meters wide, aluminum rails, and precision translation stages with positioning accuracy of 10 microns. Figure 4 shows a view of the complete assembly from the upstream camera position. Once the target was aligned and leveled, the precision translation stages were used to move the target upstream and downstream so calibration images could be obtained at the focal plane and on either side of it.

After performing the calibration, seeding the flow became the primary focus. An attempt was made to seed the flow with polystyrene latex spheres (PSL) but the particle density was not adequate. As such, PSL was abandoned in favor of smoke generators. The smoke generators use a mineral oil based mixture to produce polydisperse particles ranging in diameter from 0.25 microns to over 1.5 microns. A single smoke generator was located downstream of the test section where smoke could be injected into the diffuser and travel around the tunnel circuit before entering the test section. A 15 second burst of smoke was sufficient to obtain good correlation across the entire image. Generating smoke for periods longer than 15 seconds produced much higher seed density which resulted in a lower signal to noise ratio and multiple peaks in the image correlations.

Sample Results: Body Only

In order to evaluate the capabilities of the system in a relatively simple environment, the first measurements were made in the wake of the body alone. Data were collected in a plane measuring 0.65 meters high by 1.41 meters wide located 0.305 meters downstream of the body (X/L = 0.89) at freestream velocities of 51.44 m/s and 72.02 m/s. The position of the measurement plane relative to the body is shown in Figure 5 along with the reference point from which all distances were determined. At the 51.44 m/s condition, 100 images were acquired with the body set at 0, 2, and -5 degrees angle of attack with 0 degrees sideslip and at 0 degrees angle of attack with -5 degrees sideslip. At the 72.02 m/s condition, 100 images were acquired with the body set at -0.54 degrees angle of attack and 0 degrees sideslip. At each condition, the 100 image pairs were acquired and stored in approximately 10 minutes.

The images were processed using a fast Fourier transform correlation algorithm[17] and a 64 pixel by 64 pixel interrogation window with 50% over sampling or overlap. These settings were selected after attempts to process the data using smaller interrogation windows and higher overlap produced voids or spurious vectors in parts of the images where particles were not sufficiently exposed. In the dewarped images, each pixel on the camera sensor covered an area 0.290 mm by 0.290 mm in the measurement plane, which corresponds to a spatial resolution of 18.56 mm by 18.56 mm for this interrogation window size. Figure 6a shows color contours of the average streamwise velocity component measured at 51.44 m/s for $\alpha = 0°$ and $\alpha = -5°$. For these and all remaining data plots pertaining to the Slowed-Rotor Compound Helicopter test, streamwise distances have been normalized by the length of the body (1.757 meters), spanwise and vertical distances have been normalized by the half span of the wing (0.914 meter), velocities have been normalized using the freestream velocity and vorticity has been normalized using the freestream velocity and half span of the wing. At each condition, the LFPIV system successfully captures the wake behind the body and the vortex sheet from the inboard section of the wing including the wake of the engine nacelle. The tip vortex is only

slightly visible in the velocity contour plot but clearly identified in the contour plot of the streamwise vorticity shown in Figure 6b along with vortices emanating from the horizontal tail. The streamwise component of vorticity was computed using the following equation:

$$\omega_X = \frac{\partial W}{\partial Y} - \frac{\partial V}{\partial Z}.$$

For these fuselage angles of attack, the horizontal tail is at a slightly negative angle of incidence so the vortex from either side of the tail and the adjacent wing tip vortex spin in opposite directions.

To assess the relative accuracy of the system, LFPIV results were compared with measurements from a multi-hole probe. Figures 7a and 7b show contours of streamwise velocity and vorticity obtained using LFPIV and the QWSS at 51.44 m/s, ($\alpha = \beta = 0°$). Both measurement techiques capture the highly distorted wake behind the fuselage and the vortex sheet from the wing. The location and strength of the wing tip and horizontal tail vortices are also comparable for both techniques. Additional comparisons were performed by extracting data from LFPIV and QWSS results at Y/b = 0.00, 0.30, 0.60, and 0.90 to produce the streamwise and vertical velocity profiles shown in Figure 8. The profiles show remarkable agreement in terms of magnitude and shape even in the wake behind the body at Y/b = 0.0. The streamwise velocity profiles show some differences in magnitude in the wake of the wing (Z/b = -0.3) at Y/b = 0.30 and Y/b = 0.60 and near the wing tip vortex at Y/b = 0.90. Differences are also noted in the peak vertical velocity measured at this location and may be due to spatial averaging.

Sample Results: Body and Rotor

After completing measurements on the body alone, IRTS and the rotor were installed. Data were collected using the LFPIV system at the same downstream location (X/L = 0.89) and upstream of the vertical tail (X/L = 0.53) at 51.44 m/s and 72.02 m/s. The fuselage angle of attack was set to -0.54 degrees and the rotor shaft angle was set to -5 degrees with a collective of 12 degrees. The nominal rotation speeds of the rotor were 1870 rpm (31 Hz) and 2200 rpm (34 Hz) corresponding to hover tip Mach numbers of 0.51 and 0.60, respectively. At X/L = 0.89, a minimum of 250 images were acquired in a plane measuring 0.65 meters high by 1.41 meters wide at rotor blade azimuth positions of 1.1°, 22.5°, 45°, 77.3°, and 90°. At X/L = 0.53, 150 images were acquired every 6 degrees between Ψ = 1.1° to Ψ = 90°. The LFPIV system was synchronized with rotor shaft position using a Rotor Azimuth Synchronization Program (RASP) developed at NASA Langley. The RASP was used to produce TTL pulses at sub-harmonics of the 1/rev signal to drive the lasers at a suitable repetition rate and trigger the cameras to acquired images at specific blade azimuth positions.

For initial runs with this configuration, 800 image pairs were acquired to determine the nominal data rate and estimate the number of images required for statistical convergence. The 800 image pairs were acquired at the full frame rate of the camera (4.63 Hz) and stored in approximately 36 minutes which equates to an approximate acquisition rate of one image pair every three seconds. To determine statistical convergence, the cumulative average was computed for each velocity component and plotted versus number of images at points within the measurement plane where the root mean square of the velocity was found to be high. From this analysis, it was determined that 200 images were sufficient for the mean velocities to converge to a single value.

Prior to making measurements at X/L = 0.89, the rotor wake was visualized using smoke and a laser light sheet to determine the proper position for the measurement plane for capturing as much of the rotor wake as possible. Figure 9 shows the streamwise and spanwise position of the measurement plane relative to the model. The reference point from which all distances were determined is shown between the body and the rotor. In Figures 10a and 10b, contours of streamwise velocity and vorticity obtained for Ψ = 45° and Ψ = 90° reveal the interaction that occurs between the body and rotor wakes at the two rotor blade azimuths. The effects of this interaction are most noticeable in the upper portion of the wake in Figure 10a between Y/b = -0.3 and Y/b = 0.4. The vorticity contours show differences in the wake structure from prior blade passages and position of the blade tip vortex which passes through the central part of the measurement plane (Y/b = 0.27, Z/b = 0.105) at Ψ = 45° and then moves outboard as the blade advances to Ψ = 90°. The rotor wake has no apparent effect on the vortices from the wing tip and horizontal tail.

For the measurements at this location, the spatial resolution of the LFPIV system was adequate to capture the blade tip vortex but not

sufficient to fully resolve important characterisitics such as the velocity distribution through the core and vortex strength. To improve spatial resolution, a smaller interrogation window and more overlap can be used provided that the particles are sufficiently exposed in the images. The system can also be configured with lenses having longer focal lengths to reduce the field-of-view and increase the number of pixels over a given area. Another approach is to use a second PIV system with a smaller field of view to "zoom in" on regions of the flow where higher resolution is required. A second PIV system was setup during this application to obtain higher resolution measurements of the wing tip vortex but synchronization problems prevented images from being recorded properly.

The second measurement plane was located upstream of the vertical tail at X/L = 0.53. Documenting the wake in this region is of particular interest and importance because the flow is highly unsteady, which can induce significant unsteady loads on the vertical tail. For this measurement plane, a 480 mm focal length lens was used to reduce the field of view to 0.381 meters high by 0.914 meters wide. Using an interrogation area size of 64 pixels by 64 pixels, the spatial resolution for this location was 12 mm by 12 mm.

Figure 11 shows the streamwise and spanwise position of the measurement plane at X/L = 0.53 relative to the model. Figures 12a and 12b show contours of streamwise velocity and vorticity measured at azimuths of $\Psi = 5.98°$ and $\Psi = 48.16°$, respectively. The contour plots in Figure 12a highlight the interaction of the body and rotor wakes near the vertical tail. The blank region in the lower left hand corner of the figure is the portion of the measurement plane that was blocked by the vertical tail in the view from the downstream camera. At $\Psi = 5.98°$, the lowest velocities occur in two separate regions: one above and to the left of the tail at Z/b = 0.22 and one centered on the tail at Z/b = 0.06. As the blade advances to $\Psi = 48.16°$, these low velocity regions have merged but remain centered near the tail. The vorticity contours in Figure 12b show the corresponding position of the blade tip vortex and other features of the rotor wake from prior blade passages. The non-circular shape of the blade tip vortex is due to the measurement plane not being perpendicular to the vortex trajectory. Also, the instantaneous vortex core positions were not aligned before computing the average vorticity so vortex wandering will make the vortex appear larger than it actually is.

To validate the LFPIV measurements upstream of the tail, a two-component LDV system was used to measure streamwise and vertical velocity components at several spanwise locations in the measurement plane at X/L = 0.53. In Figure 13, the location of the LDV measurements are indicated by black lines superimposed over the LFPIV results. Although LDV is not a planar measurement technique, it is non-intrusive and particle-based which makes it an appropriate standard for comparison to the LFPIV system. The 14x22 LDV system is a standard fringe-based system operated in backscatter mode with a maximum focal length of approximately 7 meters. The sample volume diameter is 0.2 mm but its length in the transverse direction is approximately 5 mm due to the long focal length. At each point in the profile, data was randomly sampled for 6-9 minutes using frequency domain processors and "binned" to an azimuth range of 2.81 degrees for statistical analysis. The number of data points in each bin ranged from 15 to 75.

Figures 14a and 14b show comparisons of streamwise and vertical velocity profiles obtained using LDV and LFPIV. The LDV profiles have been produced from data collected at or near blade azimuth $\Psi = 7.03°$. LFPIV data were extracted from results at blade azimuth $\Psi = 5.98°$. The missing data below Z/b = 0.0 in the LFPIV profiles at Y/b = -0.109 is the part of the measurement plane that was blocked by the vertical tail. For the streamwise velocity profiles, both techniques show similar variations in velocity with a maximum difference of 17%. The variation in the vertical velocity profiles is much larger, especially above Z/b = 0.0 at Y/b = 0 and Y/b = -0.109, and is attributed to the unsteady flow in this region. Although not presented in this paper, the standard deviation in velocity for both LDV and LFPIV was as high as 17% at these locations compared to 7% at Y/b = 0.109.

The first application of LFPIV was challenging but clearly demonstrated the promise of the technique. Tremendous experience was gained in operating the system and numerous areas for improvement were identified. These include improving the quality of the light sheet, camera/shutter arrangement, and the calibration procedure. As an additional outcome, the data has proven to be suitable for performing initial comparisons with time-accurate computer simulations on this configuration. These comparisons are discussed in a companion paper by Allan, et al.[18]

Hover Application: Non-Intrusive GRMS Hover Test

Background

The second application of the LFPIV system was part of the Non-Intrusive GRMS Hover Test conducted with the U.S. Army to evaluate non-intrusive measurement techniques for rotorcraft testing in the Rotor Test Cell at NASA Langley Research Center. The first phase of testing focused on the use of Pressure Sensitive Paint (PSP) to measure unsteady surface pressures on the upper surface of the blade near the tip. During the second phase, LFPIV was used to document the blade tip vortex at several wake ages.

The model shown in Figure 15 consisted of a four-bladed rotor mounted on a ROBIN fuselage attached to the General Rotor Model System (GRMS)[19]. Each blade had a radius of 1.683 meters and a root chord of 0.138 meter. At 95% of the radius, the quarter chord is swept by 30 degrees which results in a tip chord of 0.083 meter. Two of the blades were instrumented with chordwise rows of unsteady pressure transducers near the tip for comparison with PSP measurements. One blade had two rows at 0.93R and 0.95R. The other had one row at 0.93R. The GRMS housed the electric motors to drive the rotor as well as two internal strain gauge balances, one for the rotor and one for the body. The GRMS was mounted on a sting that extended from a model cart which was used to adjust angle of attack and sideslip. This arrangement placed the rotor approximately 6.020 meters above the floor.

System Setup

To avoid the difficulty associated with installing system components and making adjustments at the above mentioned heights, the LFPIV system was configured so the majority of the system components could be installed and accessed from the floor. This arrangement, shown in Figure 16, places the system in forward scatter with the light sheet projecting down from above the rotor and the cameras looking upward from below the rotor. To minimize potential buffeting and vibration due to the downwash from the rotor, the cameras were mounted on stands made of aluminum rail shown in Figure 17. Each camera was positioned approximately 0.914 meters above the floor and 4.877 meters from the centerline of the rotor shaft to achieve an approximate angle of 45 degrees between the optical axes of the cameras and the center of the measurement plane. The camera heads were attached to a series of translation and rotation stages to provide the necessary degrees of freedom for adjusting the focus and Scheimflug angle. The shutter was attached directly in front of the camera head and connected to the lens with a bellows to prevent background light from reaching the sensor. The desired field of view of 1.524 meters by 0.914 meters was obtained using large format lenses with a focal length of 150 mm.

The light sheet was generated using two 1.5 Joule, Nd-YAG lasers with a repetition rate of 10 Hz and nominal beam diameter of 14 mm. The beams from the two lasers were combined and directed through a set of cylindrical lenses to help reduce the beam divergence and set the thickness of the light sheet at 10 mm. The beams were then directed to a pair of front surface mirrors which redirected the beam above the rotor. The beam was then reflected from a 60 mm cylindrical mirror to create a vertical light sheet fixed at $\Psi = 270°$. Figure 16 shows the path of the laser beam and the position of the light sheet relative to the model.

With the light sheet in place, the next step was to perform the calibration. Because of the inherent difficulty in translating a large target 6 meters above the ground, a three-dimensional target shown in Figure 18 was constructed using aluminum rail and retro-reflective dots and positioned in the measurement plane using a lifting platform. The rails with the retro-reflective targets are offset which essentially mimicked the displacement that would be achieved by translating the target. Besides being rigid and lightweight, this type of target made the calibration procedure less complicated and time-consuming.

The final step in the setup was to examine the seeding to insure uniform density throughout the measurement plane. Initially, the same smoke generator from the Slowed-Rotor Compound Helicopter test was used however the smoke was quite dense and persisted for a long period of time. Although the amount of seed and frequency of injection could be adjusted to obtain reasonable results, many of the test images when processed appeared to be in the "speckle" mode rather than "particle" mode. To obtain images in "particle" mode and improve signal quality, a portable spray system consisting of five spray nozzles was assembled to inject 1.86 micron PSL particles into the flow.

Sample Results

This section will present and discuss a sample of the results obtained during this application. Over 200 images were acquired every 10 degrees between Ψ = 280° and Ψ = 340° at thrust coefficients of 0.005, 0.007, and 0.009. The nominal RPM was 1150 (19.1 Hz) corresponding to a blade tip Mach number of 0.58. Images were also acquired at azimuths of 30, 60, 120, 150, 210, and 240 degrees to examine blade to blade differences.

Figures 19a and 19b show color contours of the average vertical velocity and vorticity for two different thrust conditions at Ψ = 280°. This was the closest position to the blade that could be achieved without the light sheet impinging on the blade near the root. In these and all remaining data plots pertaining to the hover test, all distances have been normalized by the rotor radius and are relative to the center of rotation. Velocities have been normalized using the rotor tip speed (ΩR) and the vorticity has been normalized using the rotor tip speed and rotor radius. The data were processed using a 32 pixel by 32 pixel interrogation window with 50% overlap. This equates to a physical spatial resolution of 12.96 mm by 12.96 mm and places a vector every 0.648 cm. As previously stated, the light sheet position was fixed at Ψ = 270° so the measurement plane was not normal to the vortex trajectory. As such, the shape of the blade tip vortex is slightly distorted. The velocity contours clearly show the wake contraction boundary and velocity differences associated with the outer flow and the wake regions. The contours also capture the increase in downwash as thrust is increased. The vorticity contours show one of the advantages of the LFPIV system in that the field of view is large enough to capture the tip vortex and inboard vortex sheet at several different wake ages (different blade passages) simultaneously. In addition, the instantaneous PIV frames can be used to align the vortex cores at each wake age to extract specific characteristics of the blade tip vortex such as peak vorticity and swirl velocity.

LDV was not available during this application so a 2D LFPIV system was set up and synchronized with the 3D LFPIV system to obtain redundant measurements for validating the 3D results and assessing system accuracy. Since the out-of-plane velocity component was assumed (and later confirmed) to be smaller than the in-plane velocity components, 2D PIV can be used to evaluate how well the 3D PIV system determines in-plane displacements (i.e. velocities). Since 2D PIV and 3D PIV are calibrated using different photogrammetry techniques and use different interrogation schemes to determine individual velocity components, the two measurement techniques can be considered to be essentially independent.

The 2D LFPIV system utilized a dual camera setup: one camera to acquire data near the blade tip and a second camera to acquire data near the blade root. Each camera had a resolution of 2000 pixels by 2000 pixels or 4 Mega-pixels and a maximum frame rate of 9.0 frames per second. The cameras were attached to stands and mounted on top of the model cart approximately 7.62 meters aft of the model. The field of view at this distance was 0.762 meters by 0.762 meters using a lens with 150 mm focal length. The 2D LFPIV data was processed using a 32 pixel by 32 pixel interrogation window with 50% overlap. Figure 20 shows color contours of the out-of-plane vorticity computed using data from the 2D and 3D systems for blade azimuth Ψ = 315°. The 2D results are from the camera focused near the blade tip. The results show good agreement both qualitatively and quantitatively. An additional comparison was performed by extracting data along profiles through the core of the primary blade tip vortex to produce the velocity profiles shown in Figure 21. For this comparison, the core position was determined by finding the location where the average vorticity was highest. The vortex position has not been aligned in the instantaneous PIV frames so the average velocities in the profiles may be low and the vortex core diameter may be overestimated due to spatial averaging. Also, the measurement plane is not normal to the vortex trajectory so the profiles are not symmetric about zero velocity. Nevertheless, the agreement between the 2D and 3D profiles is within 9%, even where the maximum and minimum velocities occur.

Future Development

The results from the initial applications of the LFPIV system have established its capabilities and helped identify that further improvements are necessary to achieve optimal effectiveness and efficiency. In principle, a LFPIV system should record particle images with the same quality as laboratory scale PIV systems (e.g. comparable particle densities, particle image sizes, and displacements over a sufficient range of pixels). To accomplish this, additional work must be done to improve particle

seeding and exposure, laser source and light sheet quality, and calibration of imaging optics, which all contribute to the accuracy of the system. In addition to accuracy, the LFPIV must operate in production-type facilities therefore operational efficiency is also important. The following list highlights some areas where the LFPIV system can be improved to increase accuracy, operational efficiency, and overall capability for future tests.

1. Improved resolution of flow phenomena

Although the LFPIV system was able to capture a large area, the resolution was not adequate to properly resolve areas where high gradients occur such as near a vortex core. Even if the particles are exposed sufficiently, there is a limit to what can be resolved by a single camera imaging a large area. General characteristics of the flow phenomenon such as size and shape can be captured but it would be advantageous to use multiple camera/lens systems to meet both spatial resolution and spatial coverage requirements. Another option is to double the resolution by using two separate LFPIV systems to cover the desired measurement area. In either case, the light sheet thickness has to be considered because the optimum light sheet thickness for a LFPIV system may not be optimum thickness for the smaller field of view.

2. Scanning capability

One aspect of LFPIV that directly impacts system efficiency is the time required for setup and calibration. This critical step has to be repeated each time the system is realigned or repositioned. A scanning capability which enables the camera and light sheet to translate while maintaining their position with respect to one another would be extremely beneficial. Not only would it increase the amount of data that could be acquired for a given setup and given amount of test time, but it would also make it easier to capture phenomena of interest. Often the size and position of flow structures are not known a priori so the ability to adjust the position of the system based on initial measurements is a more efficient approach, especially for highly complex flows.

3. Reference position documentation

During the second application, retro-reflective dots on the calibration target and model were imaged for photogrammetry measurements. This provided an accurate method to document the system configuration and position of the measurement plane relative to the model under wind-off conditions. Although these types of measurements can be made with conventional techniques, optical methods can now provide comparable levels of accuracy and require less time. Such a system would be especially useful when measurements are being made at several locations and should be an integral part of any LFPIV setup.

4. Distributed computer systems for acquisition and processing

The speed at which PIV images can be acquired and written to random access memory (RAM) or streamed to disk for storage is dependent on the camera frame rate, burst capture rate of the frame grabber, and the speed of the internal bus. Because images for the LFPIV system can be quite large (10 Megabytes or greater per image), a high burst rate framegrabber or separate computers for each camera may be needed to allow each camera pair to operate at its full frame rate. The large image size also has implications on image processing speed. On average, 150 images acquired using the LFPIV system can be processed in four hours using a workstation with eight processors. This equates to a processing rate of approximately 1 image every 2 minutes. While this turnaround time may be acceptable for post-processing, it may not be fast enough to provide useful data for making "real-time" decisions during the course of a test. The need to use multiple camera systems and process large amounts of data in a short period of time can possibly be addressed by using a distributed computer environment for data acquisition and reduction. This would make data readily available during the course of the test and help to determine if additional data is required or if a dataset needs to be retaken.

5. Remote monitoring and adjustment

Despite attempts to make the LFPIV system as robust as possible, the cameras, light sheet optics, laser system, and other components can become misaligned or stop working properly during testing. Sometimes diagnosing when and where the misalignment or component failure occurred can take considerable time and impact the overall test schedule and objectives. This risk can be mitigated by implementing systems to monitor major system components and perform adjustments remotely. Such systems would make it possible to identify potential problems well in

advance or in near-real time before failure occurs or data quality is affected.

6. Independent measurements for validation

For the LFPIV data to be useful and reliable, appropriate steps must be taken to better quantify its accuracy. Because the particle images do not cover the 2-3 pixels as required by most algorithms, achieving sub-pixel resolution may not be possible and may result in pixel-locking. Although uncertainty estimates can be made based on the ability of the system to resolve known displacements of a fixed target or speckle pattern, it is useful to have some type of redundant, in situ measurement to help validate and assess the LFPIV results. The use of redundant techniques must be incorporated into the test plan to facilitate data comparisons. When such techniques are not available, a calibrator or local jet may be used to produce a flow with known velocities that can then be measured using the LFPIV system. This is akin to the process used to calibrate hot-wires and should be performed under wind-off conditions.

7. *Seeding*

Seeding flows for PIV is always difficult, especially in large facilities like the 14x22. While the particles need to be as large as possible for proper exposure, they must also be small enough to follow the streamlines properly. Injecting particles into the flow is perhaps the easiest part of the process but getting the particles to persist around the tunnel circuit and controlling the density are always challenging. Also, achieving proper seed density in the core of a vortex or region of reverse flow is especially difficult. Smoke generators can produce sufficient seed density for facilities the size of the 14x22 or Rotor Test Cell but the smoke tends to dissipate at high temperatures and can introduce unwanted noise in the particle images. Also, if the density gets too high, the image processing will begin correlating on speckle patterns as opposed to particles. In contrast, PSL is not as susceptible to high temperatures and provides a better signal-to-noise ratio than the smoke but does not always provide acceptable density. Further work is needed to identify the best media and methods for seeding the flow in these facilities.

Concluding Remarks

A Large Field-of-View PIV system has been developed for rotor wake diagnostics in the 14x22. Overall, the system performance has exceeded design expectations in terms of the data quality, efficiency, and accuracy. The system has been used in both forward flight and hover tests to successfully measure three components of velocity in planes as large as 1.524 meters by 0.914 meters. Although slightly smaller than the design objective, this field of view provided the proper size and resolution to capture a large portion of the wake from the fuselage, wing, and advancing side of the rotor during the forward flight test. It was also adequate to capture the tip vortex and inboard vortex sheet at several wake ages during the hover application. For each of these applications, the system operation was highly efficient based on the amount of data acquired during a given wind-on period. For a typical run lasting 2.5 hours, the system was able to acquire and store over 200 images at 15 different rotor blade azimuth locations. System accuracy has been assessed by comparing velocity profiles from the LFPIV system and two pointwise techniques, a multi-hole pressure probe and an LDV. Overall, the agreement between LFPIV and the other techniques is 17% or less. LFPIV results have also been compared to 2D PIV, another planar measurement technique, and agree to within 9% or less. Despite the success of these initial applications, improvements in image quality, resolution, scanning capability, reference position documentation, image acquisition and processing, remote monitoring and adjustment, validation, and seeding could significantly increase the accuracy, efficiency, and capability of the LFPIV system for future applications.

Acknowledgements

The authors would like to thank numerous individuals for their contributions to the success of this development effort: Gloria Yamauchi and Alan Wadcock for paving the way and providing exceptional advice; Kevin Noonan, Brendan Malvorh, and Jim Hallissy for directing the test and overseeing model operations; Fred Mason and Curt Fossum for their assistance with the model and setting up the system; the ROME Group for their assistance with facility operations and setting up the infrastructure to support the system; Gary Fleming for development of the RASP which was an invaluable tool; and Susan Gorton, Anthony Washburn, and Kenneth Wright for encouragement, support, and advocacy.

References

[1]Yamauchi, G. and Young, L. "A Status of NASA Rotorcraft Research," NASA/TP -2009-215369. 2009.

[2]McAlister, K. W., Tung, C., and Heineck, J. T., "Devices that Alter the Tip Vortex of a Rotor," NASA TM-2001-209625, February 2001.

[3]McAlister, K. W. and Heineck, J. T., "Measurements of the Early Development of Trailing Vorticity from a Rotor," NASA TP-2002-211848, 2002.

[4]Martin, P. B., Leishman, J. G., Pugliese, G. J., and Anderson, S.L., "Stereoscopic PIV Measurements in the Wake of a Hovering Rotor," 56th AHS Annual Forum, Virginia Beach, VA, 2000.

[5]Heineck, J. T., Yamauchi, G. K., Wadcock, A. J., Lourenco, L. and Abrego, A. I. "Application of Three-Component PIV to a Hovering Rotor Wake," 56th AHS Annual Forum, Virginia Beach, VA, 2000.

[6]Wadcock, A. J., Yamauchi, G. K., and Heineck, J. T., "Three-Component Velocity Measurements in the Wake of a Rotor in Hover," Highlights of the Aero-Space Technology Enterprise, 2002.

[7]Wadcock, A. J., Yamauchi, G. K., Heineck, J. T., Silva, M. J., and Long, K.R., "PIV Measurements of the Wake of a Tandem-Rotor Helicopter in Proximity to a Ship," AHS 4th Decennial Specialist's Conference on Aeromechanics, San Francisco, CA, January 21-23, 2004.

[8]Silva, M. J., Yamauchi, G. K., Wadcock, A. J., and Long, K. R.: Wind Tunnel Investigation of the Aerodynamic Interaction Between Helicopters and Tiltrotors in a Shipboard Environment," AHS 4th Decennial Specialist's Conference on Aeromechanics, San Francisco, Calif., Jan. 21–23, 2004.

[9]Raffel, M., Richard, H., Ehrenfried, K., Van der Wall, B., Burley, C., Beaumier, P., McAlister, K., and Pengel, K., "Recording and Evaluation Methods of PIV Investigations on a Helicopter Rotor Model," Experiments in Fluids, Springer-Verlag, 2004, pp. 146-156.

[10]Wernet, M. P., "PIVACQ Software Manual Version 3.3," NASA Glenn Research Center, September 2007.

[11]Freeman, C. E. and Mineck, R. E., "Fuselage Surface Pressure Measurements of a Helicopter Wind-Tunnel Model with a 3.15-Meter Diameter Single Rotor," NASA TM 80051, March 1979.

[12]Gentry, Jr., G. L., Quinto, P. F., Gatling, G. M., and Applin, Z. T., "The Langley 14- by 22-Foot Subsonic Wind Tunnel: Description, Flow Characteristics, and Guide for Users", NASA Technical Paper 3008, 1990.

[13]Buning, P. G., Jespersen, D. C., Pulliam, T. H., Klopfer, W. M., Chan, W. M., Slotnick, J. P., Krist, S. E., and Renze, K. J., "OVERFLOW User's Manual Version 1.8m," Tech. Report, NASA Langley Research Center, 1999.

[14]Jespersen, D., Pulliam, T., and Buning, P., "Recent Enhancements to OVERFLOW," AIAA paper 97–0644, January 1997.

[15]Schwartz, Richard J., "ViDI: Virtual Diagnostics Interface, Volume 1 — The Future of Wind Tunnel Testing," NASA/CR-2004-212667, 2004.

[16]Kusunose, K., Crowder, J. P. and Watzlavick, R., "Wave Drag Extraction From Profile Drag Based on a Wake-Integral Method," AIAA-1999-275, 1999.

[17]Scarano, F. and Riethmuller, M., "Advances in Iterative Multigrid PIV Image Processing," Experiments in Fluids Supplemental, 29:S51–S60, 2000.

[18]Allan, B. G., Jenkins, L. N., Yao, C. S., Bartram, S. B., Hallissy, J. B., Harris, J., Noonan, K. W., Wong, O. D., Jones, H. E., Malovrh, B. D., Reise, D. G., and Mace, W. D., "Navier-Stokes Simulation of a Heavy Lift Slowed-Rotor Compound Helicopter Configuration," AHS 65th Annual Forum, Grapevine, TX, May 2009.

[19]Wilson, John C., "A General Rotor Model System for Wind-Tunnel Investigations," *J. Aircraft*, Vol. 14, No. 7, July 1977, pp. 639-643.

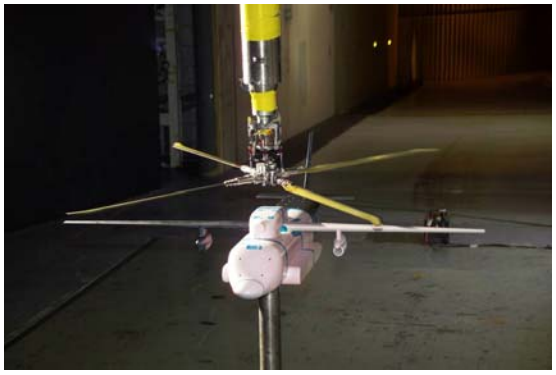

Figure 1. Slowed-Rotor Compound Helicopter model in the 14x22.

Figure 2. QWSS positioned behind the Slowed-Rotor Compound Helicopter model (body only).

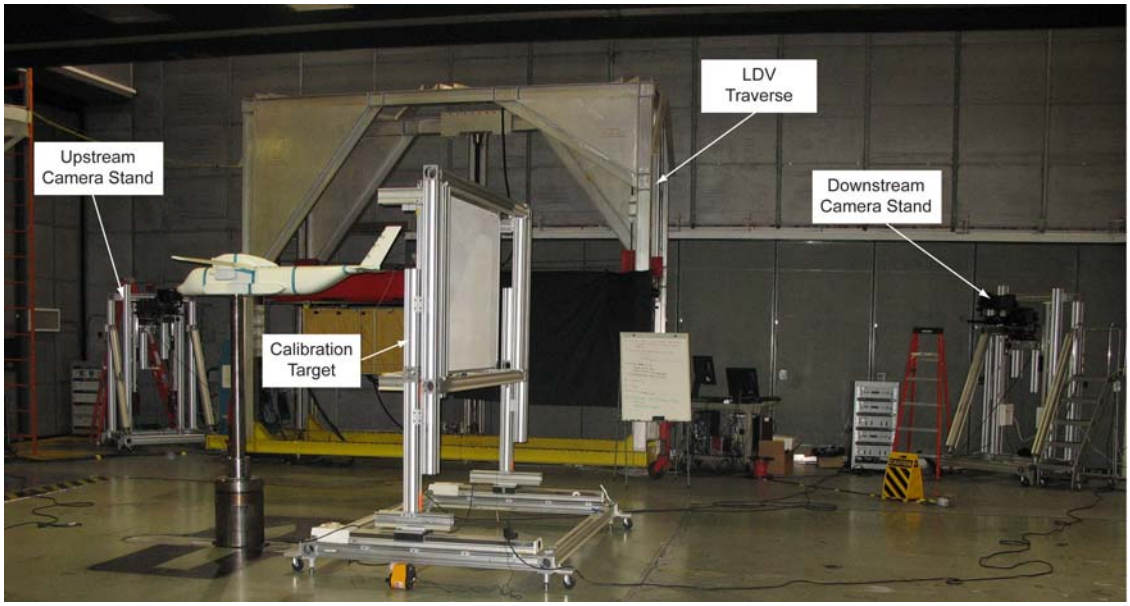

Figure 3. Slowed-Rotor Compound Helicopter Model (body alone) with PIV cameras, LDV system, and calibration target in the 14x22 with the walls raised (Note: cameras and LDV system are behind the shear layer, outside the airstream).

Figure 4. Target used to calibrate the LFPIV system.

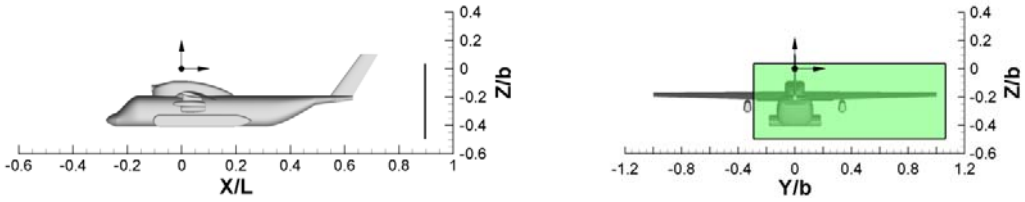

Figure 5. Measurement plane location relative to the body at X/L = 0.89 (body only)

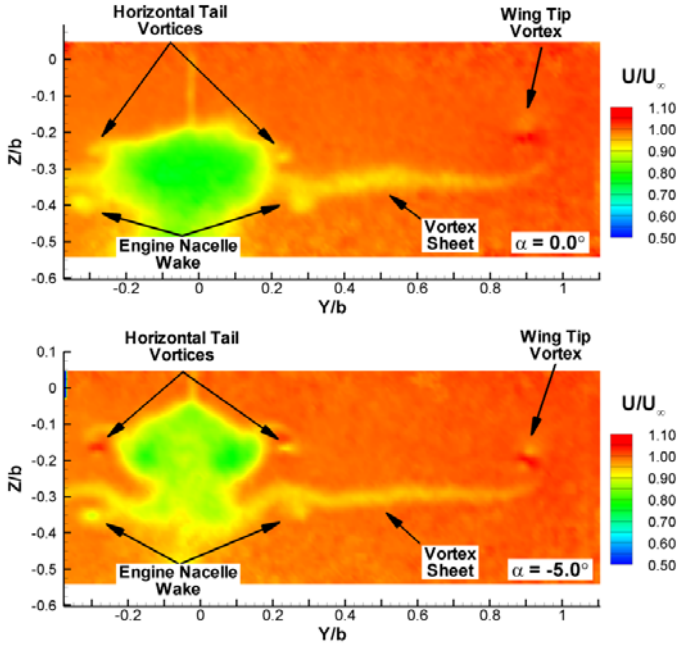

a. Streamwise velocity.

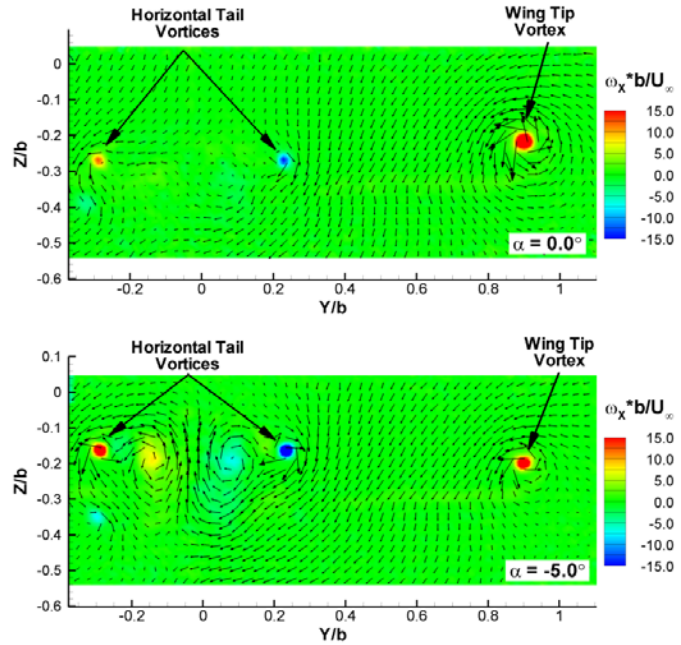

b. Streamwise vorticity.

Figure 6. LFPIV measurements of streamwise velocity and vorticity at α = 0.0° and α = -5.0° (β = 0.0°, X/L = 0.89, U_∞ = 51.44 m/s, body only).

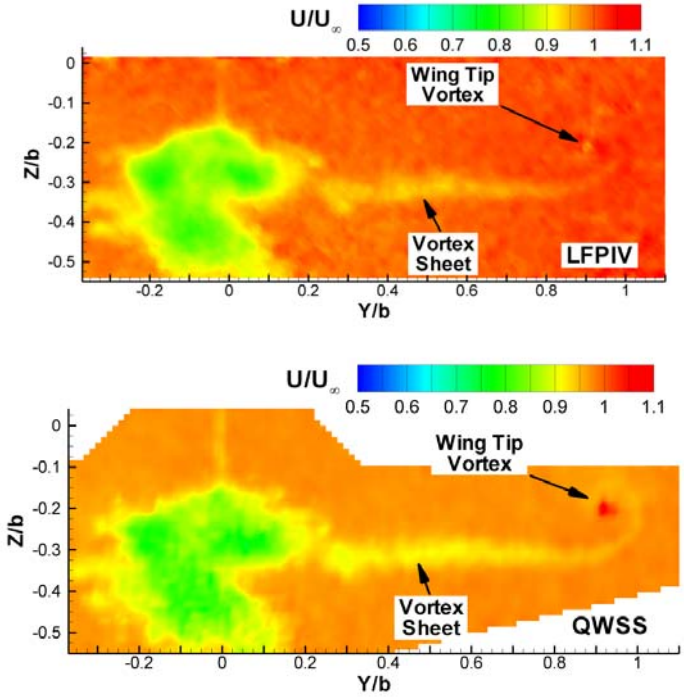

a. Streamwise velocity.

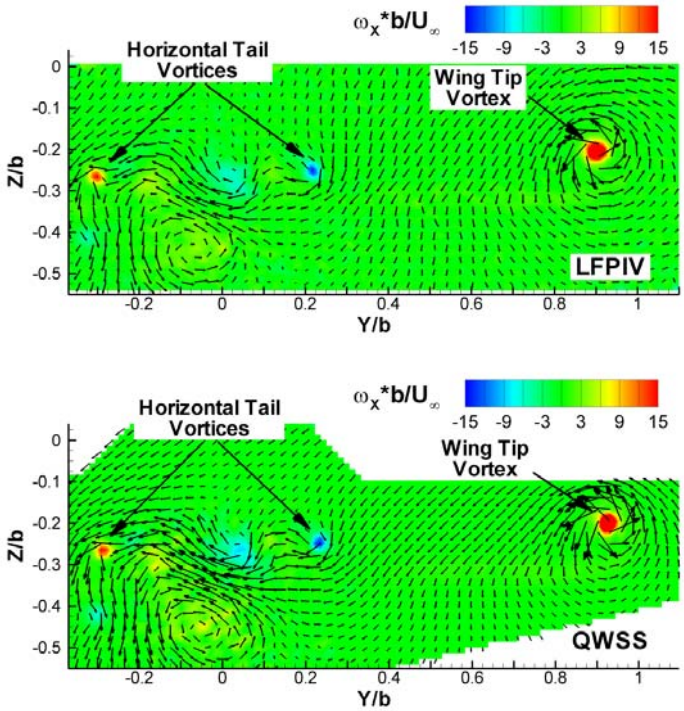

b. Streamwise vorticity.

Figure 7. Comparison between LFPIV and QWSS measurements of streamwise velocity and vorticity (α = -0.54°, β = 0.0°, X/L = 0.89, U_∞ = 72.02 m/s).

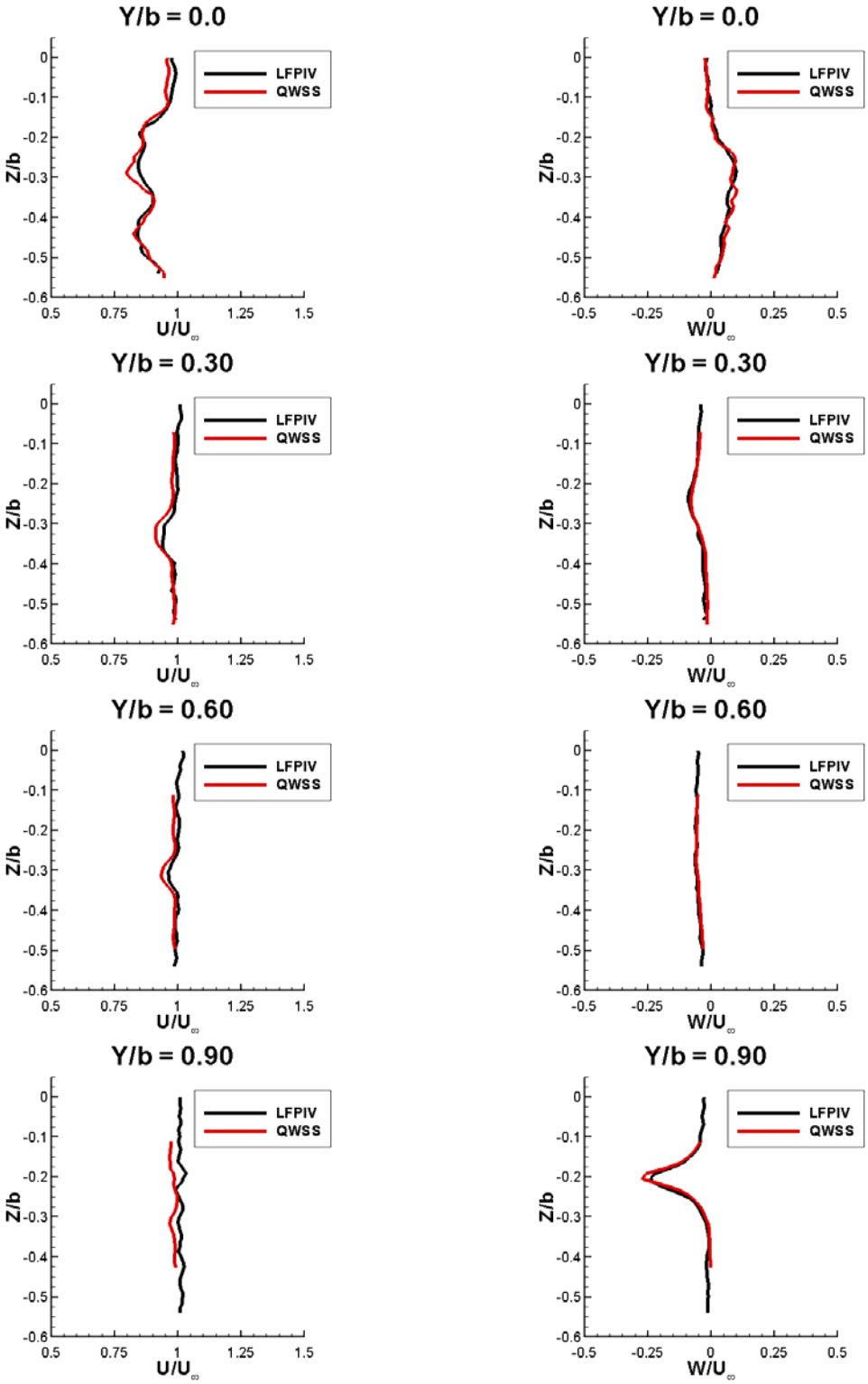

a. Streamwise velocity. **b. Vertical velocity.**

Figure 8. Comparison between velocity profiles measured by LFPIV and QWSS (α = -0.54°, β = 0.0°, X/L = 0.89, U_∞ = 72.02 m/s).

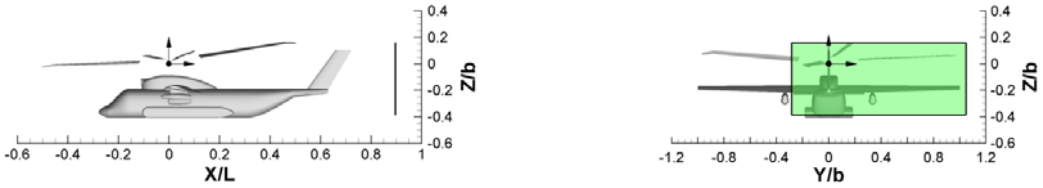

Figure 9. Measurement plane location relative to the model at X/L = 0.89 (body and rotor)

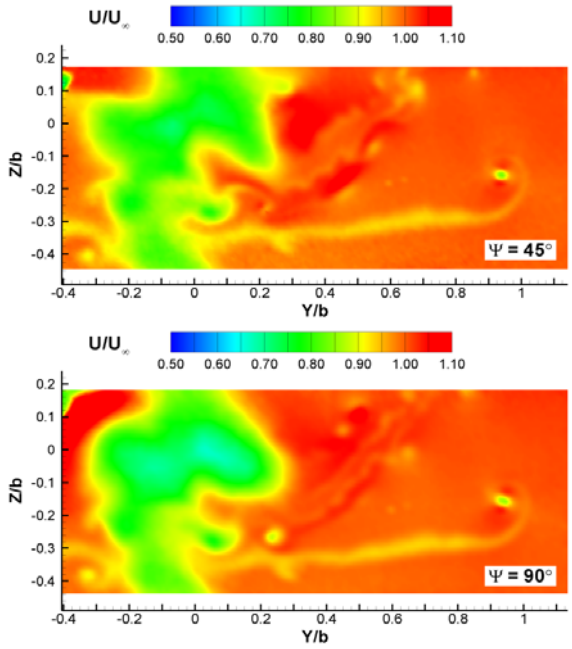

a. Streamwise velocity.

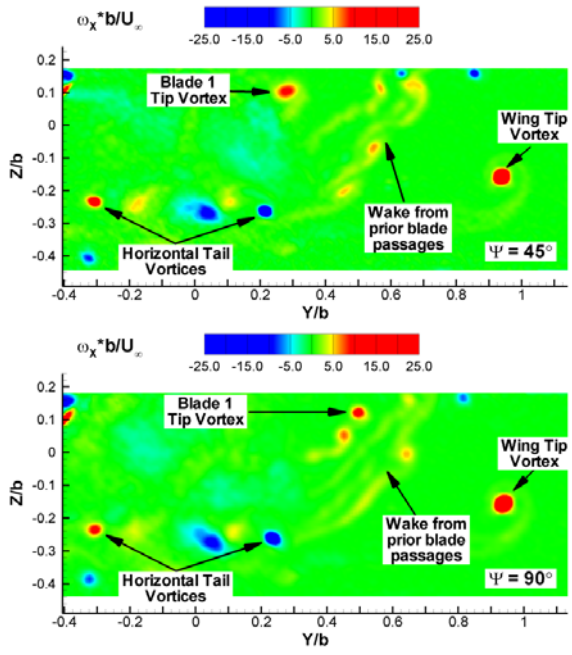

b. Streamwise vorticity.

Figure 10. LFPIV measurements of streamwise velocity and vorticity at Ψ = 45° and Ψ = 90° (α = -0.54°, β = 0.0°, X/L = 0.89, U_∞ = 72.02 m/s, body and rotor).

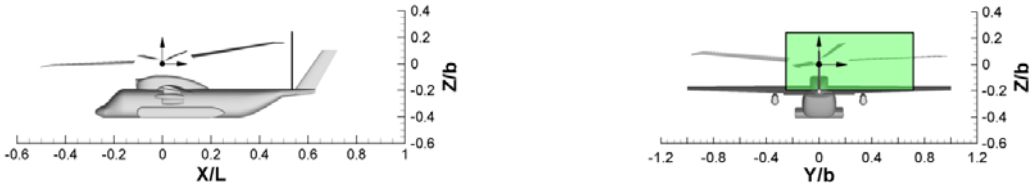

Figure 11. Measurement plane location relative to the model at X/L = 0.53 (body and rotor).

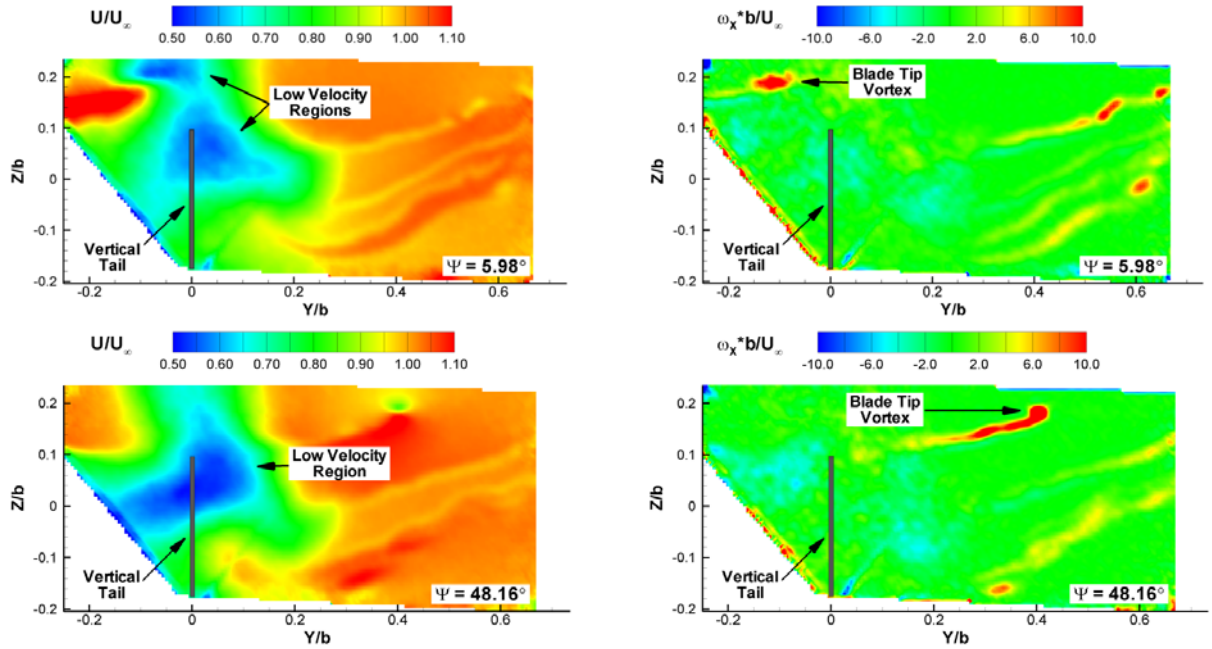

a. Streamwise velocity. **b. Streamwise vorticity.**

Figure 12. LFPIV measurements of streamwise velocity and vorticity at Ψ = 5.98° and Ψ = 48.16° (α = -0.54°, β = 0.0°, X/L = 0.53, U_∞ = 72.02 m/s, body and rotor).

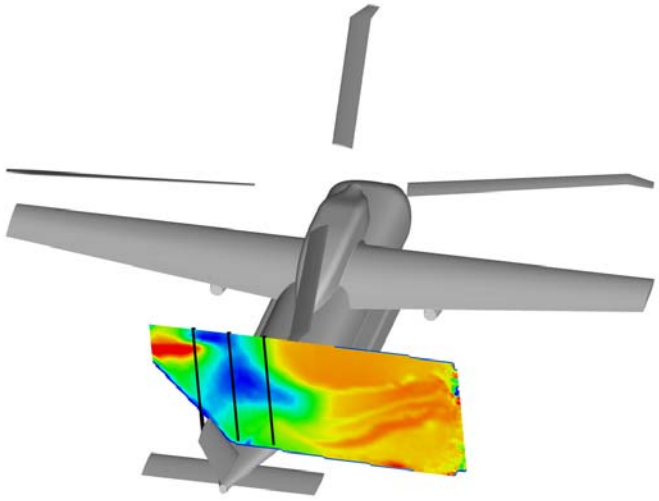

Figure 13. Location of velocity profiles used for LFPIV and LDV comparison.

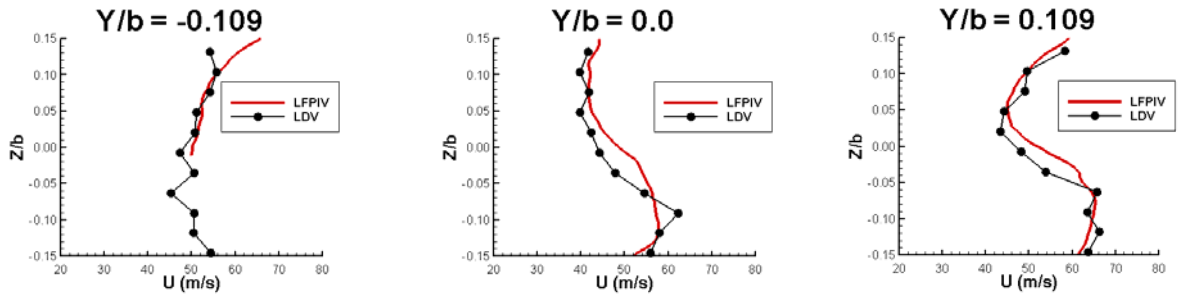

a. Streamwise velocity.

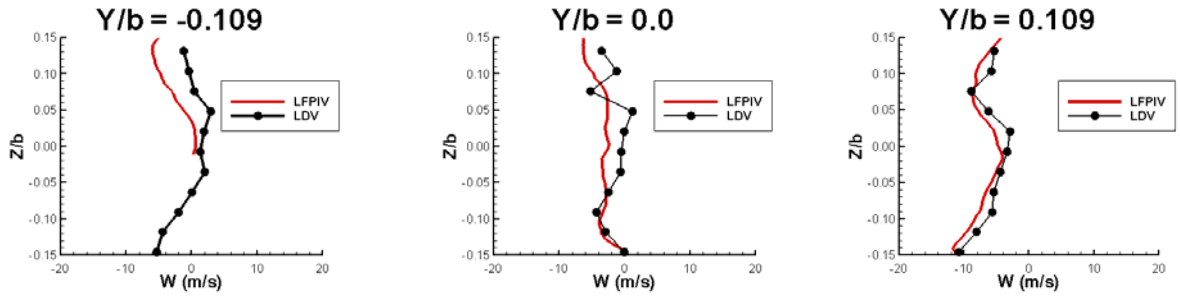

b. Vertical velocity

Figure 14. Comparison between velocity profiles measured using LDV and LFPIV (Ψ = 5.98°, α = -0.54°, β = 0.0°, X/L = 0.53, U_∞ = 72.02 m/s, body and rotor).

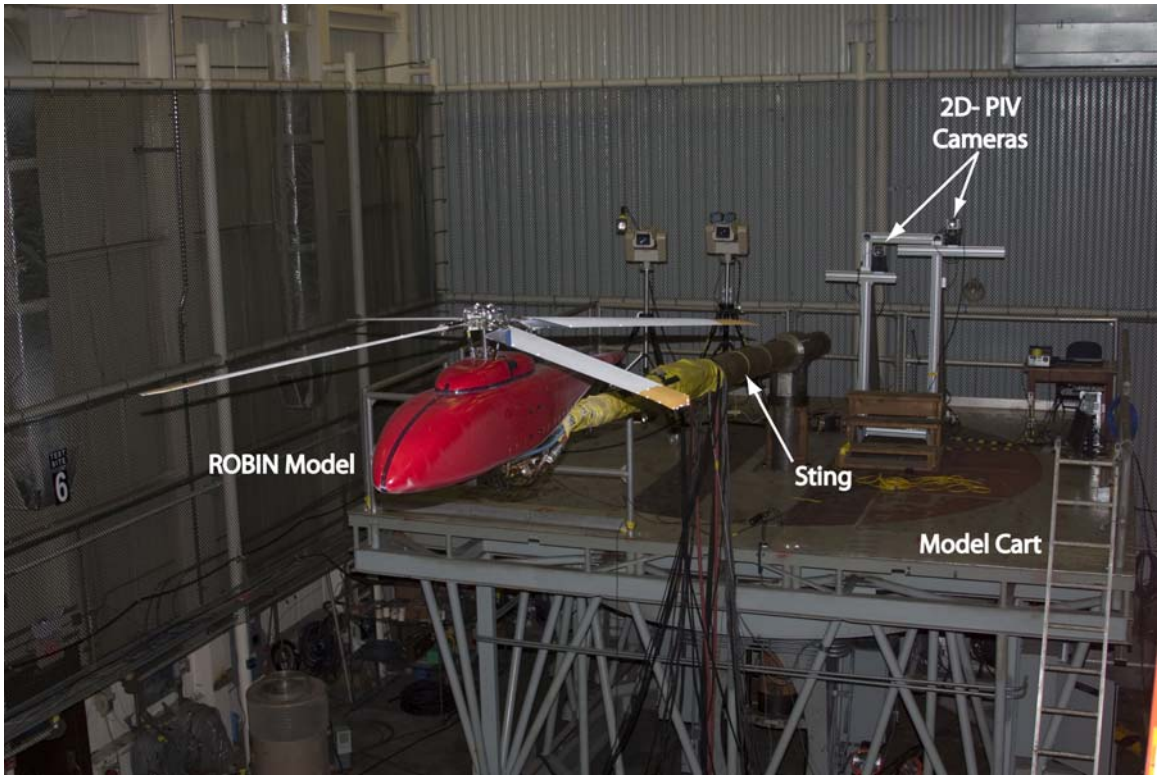

Figure 15. Model configuration used in the Non-Intrusive GRMS Hover Test.

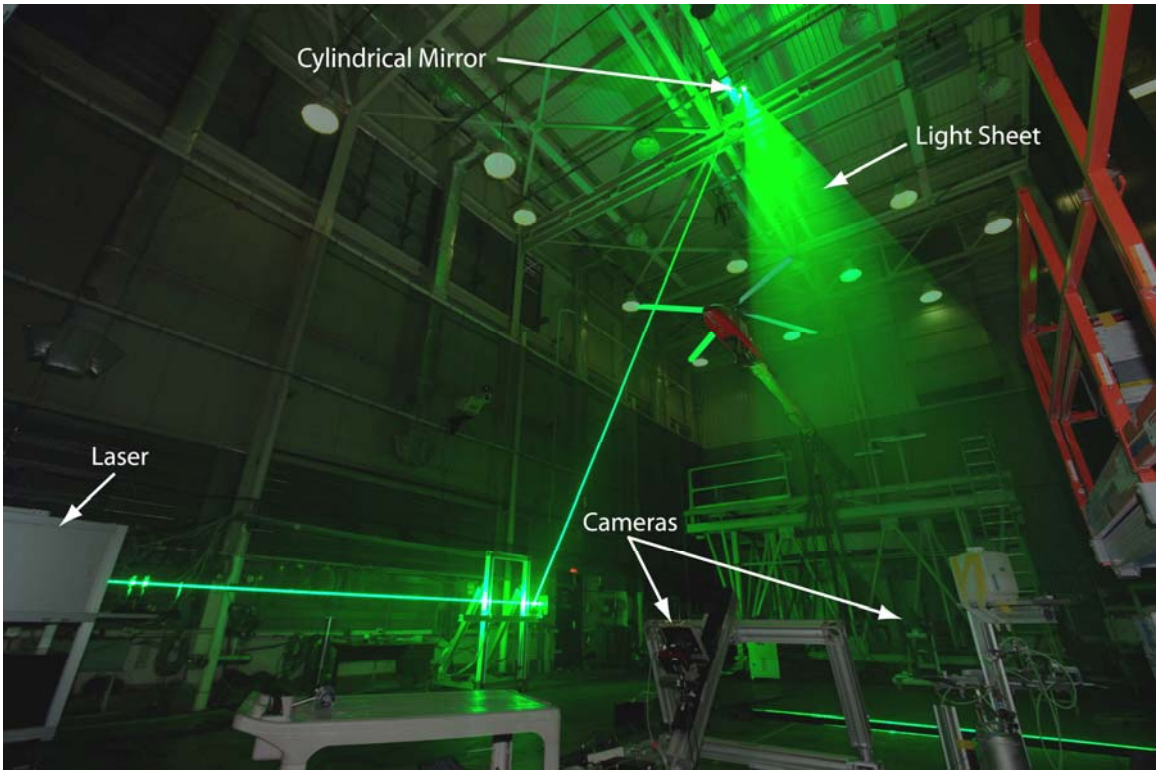

Figure 16. LFPIV setup for the Non-Intrusive GRMS Hover Test.

Figure 17. Camera stand and arrangement on optical rail.

Figure 18. Three-dimensional calibration target positioned in measurement plane.

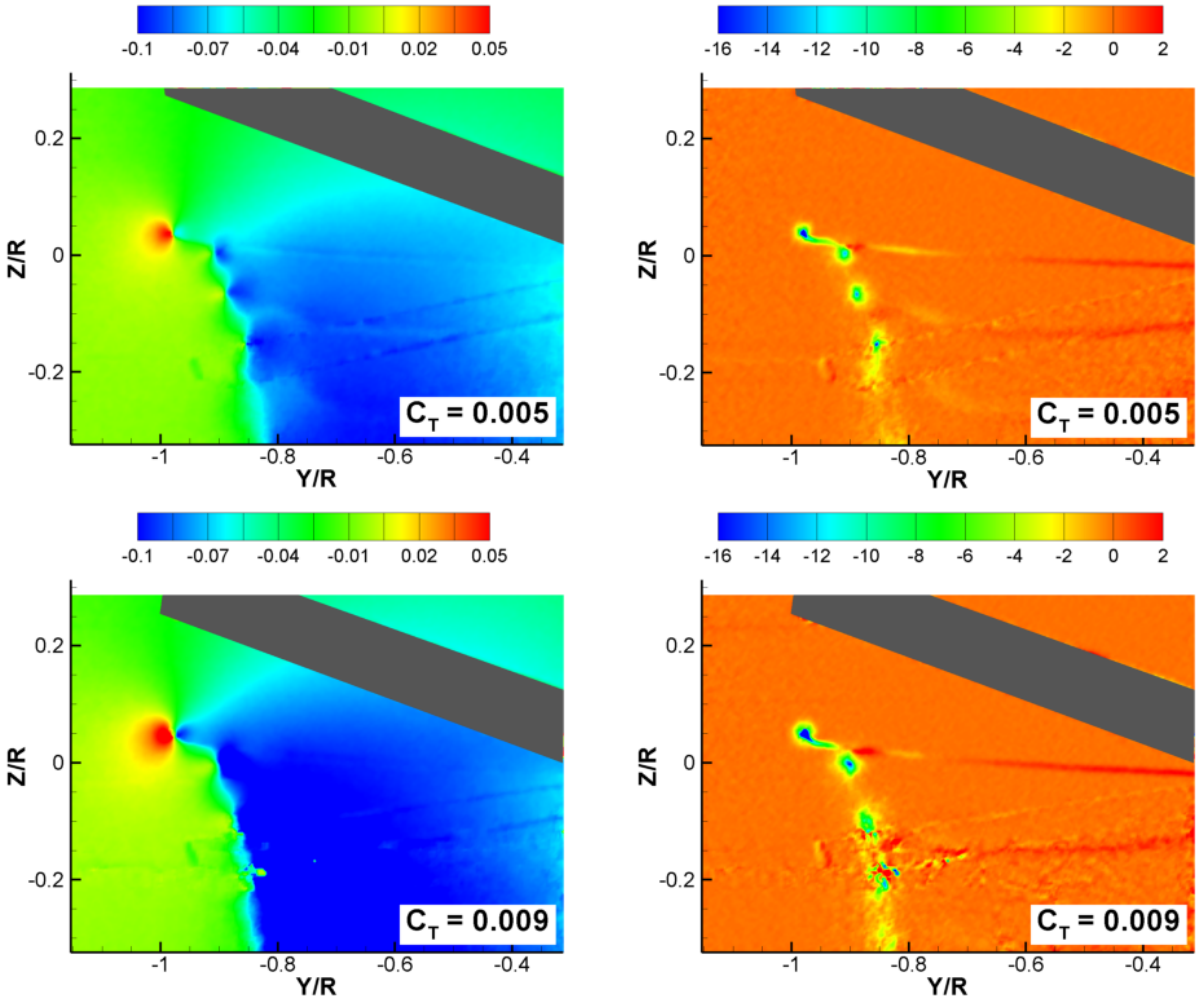

a. Vertical velocity. **b. Out-of-plane vorticity.**

Figure 19. Comparison of vertical velocity and out-of-plane vorticity at different thrust conditions (Ψ = 280°, M_{tip} = 0.52).

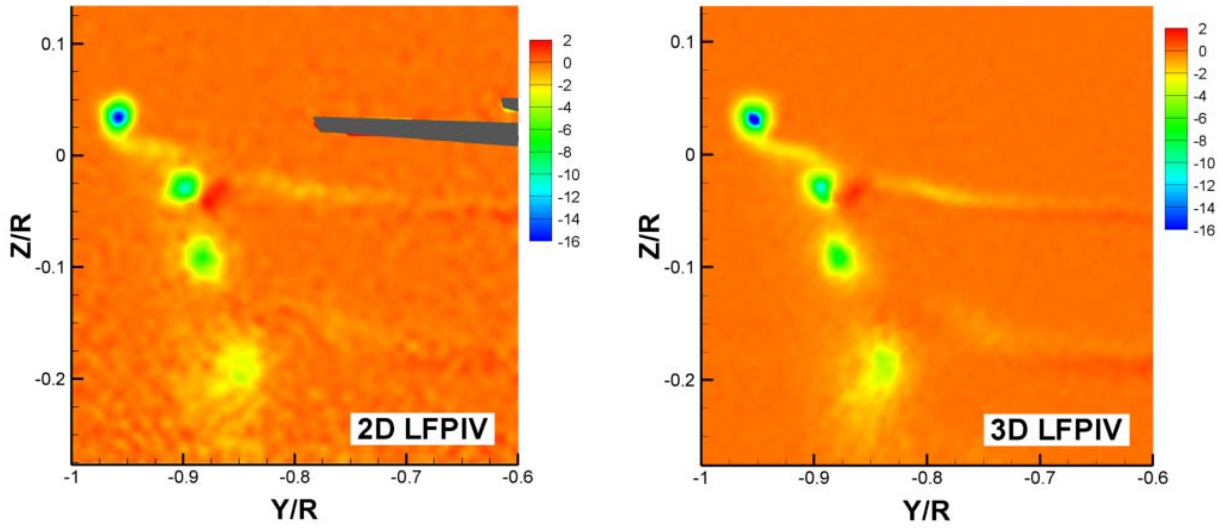

Figure 20. Comparison between 2D and 3D LFPIV measurements of out-of-plane vorticity ($\Psi = 315°$, $M_{tip} = 0.52$, $C_T = 0.005$).

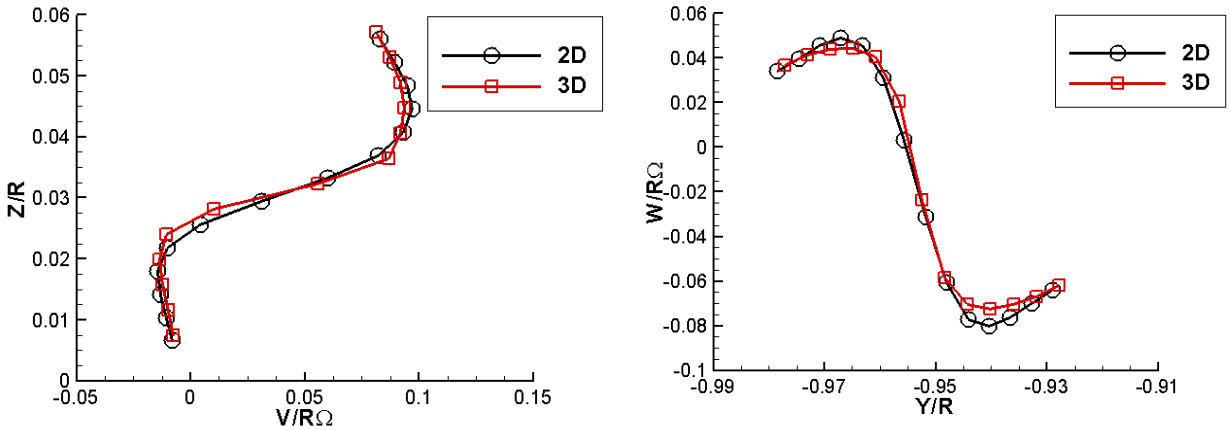

a. Spanwise velocity **b. Vertical velocity**

Figure 21. Comparison between 2D and 3D LFPIV velocity profiles through the core of the primary vortex ($\Psi = 315°$, $M_{tip} = 0.52$, $C_T = 0.005$).